

Magnetic anisotropy of Co^{2+} as signature of intrinsic ferromagnetism in ZnO:Co

P. Sati,¹ R. Hayn,¹ R. Kuzian,² S. Régnier,¹ S. Schäfer,¹ A. Stepanov,¹
C. Morhain,³ C. Deparis,³ M. Laügt,³ M. Goiran,⁴ and Z. Golacki⁵

¹Laboratoire Matériaux et Microélectronique de Provence, associé au CNRS,
Case-142, Université d'Aix-Marseille III, 13397 Marseille Cedex 20, France

²Institute for Materials Science, Krzhizhanovskogo 3, 03180, Kiev, Ukraine

³Centre de Recherche sur l'Hétéro-Epitaxie et ses Applications-CNRS, 06560, Valbonne Sophia-Antipolis, France

⁴Laboratoire National des Champs Magnétiques Pulsés, 31432, Toulouse, France

⁵Institute of Physics, Polish Academy of Sciences, Al. Lotnikow 32/46, 02-668, Warsaw, Poland

We report on the magnetic properties of thoroughly-characterized $\text{Zn}_{1-x}\text{Co}_x\text{O}$ epitaxial thin films, with low Co concentration, $x = 0.003 - 0.005$. Magnetic and EPR measurements, combined with crystal field theory, reveal that isolated Co^{2+} ions in ZnO possess a strong single ion anisotropy which leads to an "easy plane" ferromagnetic state when the ferromagnetic Co-Co interaction is considered. We suggest that the peculiarities of the magnetization process of this state can be viewed as a signature of intrinsic ferromagnetism in ZnO:Co materials.

PACS numbers: 71.20.Be, 75.30.Gw, 76.30.Fc

Spintronics, an emerging branch of micro- and nanoelectronics which manipulates the electron spin rather than its charge, has need for spin polarization components. In most spintronic devices, *metallic* ferromagnetic (FM) materials are used to this end. However the physics of metal-semiconductor injection is incompatible with the concept of semiconductor devices, preventing their application [1]. A suitable solution would be a FM semiconductor at room-temperature.

The magnetic properties of diluted magnetic semiconductors are due to the substitution of cations by transition-metal (TM) ions, and have been extensively studied for at least five decades [2]. Co-doped ZnO - a possible candidate for high- T_c FM semiconductors - has attracted much interest from both theoretical and experimental points of view. Yet, there is an ongoing debate about its magnetic properties. Early theoretical studies using the local spin density approximation (LSDA) for $\text{Zn}_{1-x}\text{Co}_x\text{O}$ found it to be a FM semimetal [3]. Contrary to this, more recent LSDA calculations [4, 5] on large supercells detected a competition between FM and anti-ferromagnetic (AFM) interactions, *i.e.* an AFM or spin-glass groundstate.

Experimentally, high- T_c FM phases in $\text{Zn}_{1-x}\text{Co}_x\text{O}$ ($x = 0.1-0.25$) were found in thin films produced by pulsed laser deposition [6], by the sol-gel method [7], and by rf magnetron co-sputtering [8]. They were also found in bulk single crystals prepared by implantation [9]. Controversially, *AFM correlations between TM ions and the absence of any FM bulk phases* were observed in $\text{Zn}_{1-x}\text{Co}_x\text{O}$ ($x = 0.005-0.15, 0.2$) samples fabricated by precursor decomposition [4], in polycrystalline powder samples [10] as well as in thin films [11].

In this rather contradictory situation a major question which arises is whether a reliable identification of an intrinsic FM phase of ZnO doped by Co is possible at all.

Here we address this question on both experimental

and theoretical grounds. We argue that such an identification requires a thorough examination of the magnetic properties of Co^{2+} ions in the ZnO lattice, and in particular the magnetic anisotropy of cobalt. By EPR and magnetic measurements, we first prove that Co^{2+} , which has a spin $S = 3/2$, shows a huge single ion anisotropy of DS_z^2 type, with $D = 2.76 \text{ cm}^{-1}$. We then validate this result theoretically by combining crystal field theory with an estimate of the crystal field parameters. Theory and experiment clearly demonstrate that Co substitutes Zn in our samples. Finally, using a simple model, we show that a FM ZnO:Co would be an "easy plane" ferromagnet exhibiting a peculiar magnetization process which offers a simple and reliable way to identify the intrinsic FM phase of ZnO:Co .

We focus on the magnetic anisotropy of isolated cobalt in ZnO and present details of the magnetic properties of epitaxial thin films with very low Co concentration varying from $x=0.003$ to $x=0.005$ [12]. The $1\mu\text{m}$ thick samples were grown on sapphire substrate by plasma-assisted MBE. 2D growth is achieved for growth temperature of 560°C , *i.e.* 50°C higher than the optimal growth temperature used for ZnO, resulting in streaky RHEED patterns. For this range of Co composition, the rocking curve FWHMs are in the range of $\omega \sim 0.15^\circ$ along (002), (-105) and (105). The low ω values measured both for (-105) and (105), as well as their similarity, indicate a large column diameter, close to $1\mu\text{m}$. The c-axis of the wurtzite structure is perpendicular to the film plane. The conductivity of the films is *n*-type, with residual carrier concentrations $n_e < 10^{18} \text{ cm}^{-3}$, a doping level well below the Mott transition.

Neglecting the hyperfine interaction, the 4A_2 ground-state of Co^{2+} at a tetrahedral site of the ZnO host lattice is described by the following $S = 3/2$ spin Hamiltonian [13]

$$\hat{H}_{spin} = \mu_B g_{\parallel} H_z S_z + \mu_B g_{\perp} (H_x S_x + H_y S_y) + DS_z^2. \quad (1)$$

The magnetic state of Co^{2+} can thus be parameterized by only three constants : the two g -factors, g_{\parallel} ($H \parallel c$) and g_{\perp} ($H \perp c$), and the zero-field splitting constant D . Henceforth, we will use (1) with the values inferred from our experiments (see below), namely $g_{\parallel} = 2.236$, $g_{\perp} = 2.277$ and $D = 2.76 \text{ cm}^{-1}$, to compute (i) the magnetization and the magnetic susceptibility of $\text{ZnO}:\text{Co}$ in a simple statistical model of an ensemble of independent spins ; (ii) the angular and field dependences of the EPR spectra ; (iii) the magnetization of small FM clusters.

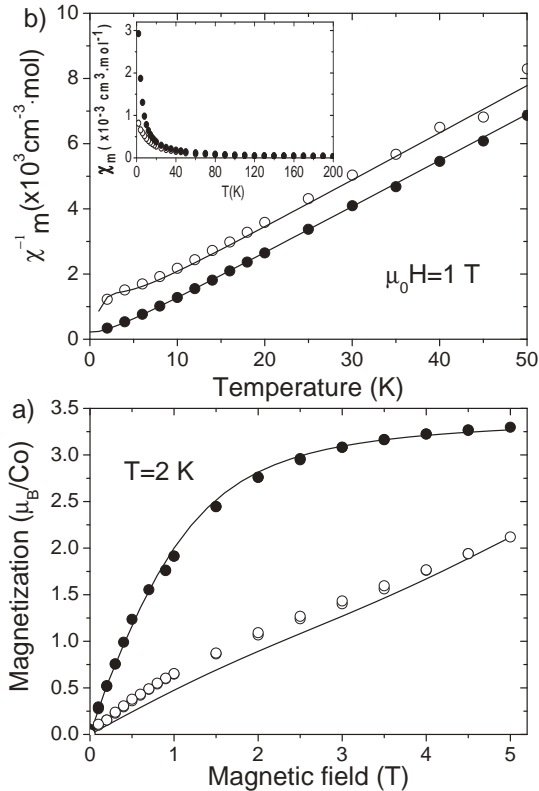


FIG. 1: a) Field dependence of magnetization for a $\text{Zn}_x\text{Co}_{1-x}\text{O}$ sample with $x=0.0028$ at $T=2\text{K}$. b) Inverse of the magnetic susceptibility for the same sample *vs* temperature at $\mu_0 H=1 \text{ T}$; the inset shows $\chi(T)$. Full and open circles are experimental data for $H \perp c$ and $H \parallel c$, respectively. Solid lines are computed according to the model discussed in the text.

First, we discuss the results of the magnetic measurements of thin $\text{ZnO}:\text{Co}$ films. The substrate was cut into thin rectangular platelets of 3 by 3 mm^2 . In each experiment, up to 10 platelets were piled up to increase the paramagnetic component of the signal. In addition, undoped ZnO films, deposited on the same sapphire substrate, were examined. The latter films served as a reference of the diamagnetic contribution of the measured signal. Measurements were performed using a Quantum Design MPMS XL magnetometer between 300K and 2K in magnetic fields up to 5 T. The field dependence of the magnetization taken at 2K and the temperature depen-

dence of the inverse of the magnetic susceptibility measured at 1 T for a $\text{Zn}_x\text{Co}_{1-x}\text{O}$ sample with $x = 0.0028$, for two orientations of the magnetic field, $H \perp c$ and $H \parallel c$, are shown in Figs. 1a and 1b, respectively.

As is clear from Fig. 1, both the magnetization and the susceptibility curves reveal a significant magnetic anisotropy. This anisotropy can be referred to as being of an "easy plane" type; *i.e.* for a given magnetic field H , the magnetization $M \perp c$ is greater than $M \parallel c$. As expected, the susceptibility curves show a paramagnetic behavior. Their deviation from a Curie law finds a natural explanation in a $S = 3/2$ model with a single ion anisotropy, where the only adjustable parameter is the concentration of Co^{2+} ions.

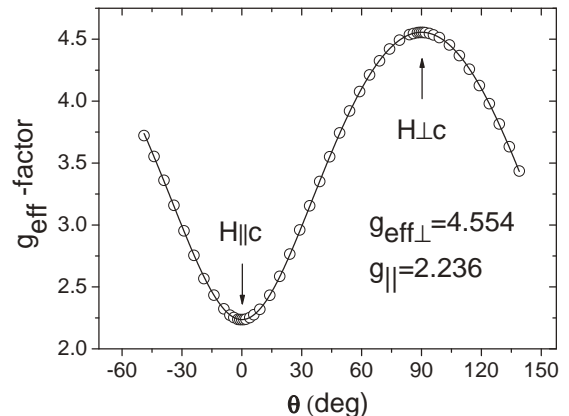


FIG. 2: Angular dependence of the effective g -factor of Co^{2+} . $\theta = 0$ corresponds to $H \parallel c$. The open circles are the experimental data; the solid line is a fit based on Eq.1.

We now turn to the results of low-frequency EPR. An EMX Bruker spectrometer was used to collect spectra in the X-band ($\nu = 9.4 \text{ GHz}$) and in the temperature range 4–300 K. A single line with a partly resolved hf structure for $H \parallel c$ was observed below $\sim 100 \text{ K}$. This clearly indicates that $D \gg h\nu$. As the temperature is lowered to 4 K, the line intensity increases monotonically, and roughly follows a simple Curie law, $\sim 1/T$, indicating that the observed EPR signal is due to the low-lying doublet $S_z = \pm 1/2$ of a $S = 3/2$ ground-state manifold [14]. Note that the latter observation also allows us to determine the sign of D , $D > 0$.

In Fig. 2 the angular dependence of the apparent (effective) g -factor of Co^{2+} in the ZnO lattice is shown, θ being the angle between the c -axis and the applied field H . The extracted values, $g_{\parallel} = 2.236$ and $g_{\text{eff}\perp} = 4.554$, are very close to those obtained previously for single crystals [14] and thin films [15] of $\text{ZnO}:\text{Co}$. The measured $g_{\text{eff}\perp}$ can be assigned to the lowest Co^{2+} doublet, yielding $g_{\text{eff}\perp} \simeq 2g_{\perp}(1 - (3/64)(h\nu/D)^2)$ for $D \gg h\nu$ [16], which with reasonable accuracy reduces to $g_{\perp} = g_{\text{eff}\perp}/2$. The above results also suggest that the Zeeman part of the Co^{2+} spin Hamiltonian is practically isotropic ($g_{\parallel} \simeq g_{\perp}$),

and hence cannot be responsible for the magnetic anisotropy of ZnO:Co. We therefore need more information about the zero-field splitting constant D which, according to the temperature dependence of the X-band EPR signal, can be estimated to $2D = 5.5 \pm 0.3 \text{ cm}^{-1}$ [14].

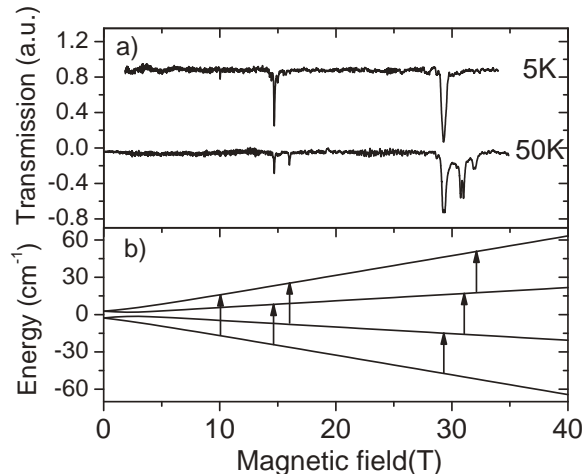


FIG. 3: a) Transmission EPR spectra of ZnO:Co taken at $\lambda = 305 \mu\text{m}$ and $\theta = 63^\circ$. b) Energy-level splitting of Co^{2+} in magnetic field at $\theta = 63^\circ$ computed according to Eq.1. The vertical arrows indicate the observed EPR transitions.

We have undertaken high-frequency EPR measurements on $\text{Zn}_{1-x}\text{Co}_x\text{O}$ ($x = 0.01 - 0.02$) single crystals in a large range of wavelengths $\lambda = 3\text{mm} - 0.3\text{mm}$. Magnetic fields up to 35 T were provided by the pulsed field facility in Toulouse. Representative transmission EPR spectra of ZnO:Co taken at the shortest wavelength ($\lambda = 305 \mu\text{m}$) are displayed in Fig. 3, together with the computed energy level splitting. The observation of the "forbidden" transitions with $\Delta m = \pm 2$ and $\Delta m = \pm 3$ confirms the presence of a large zero-field splitting term in the spin Hamiltonian. Most importantly, these experiments allowed us to measure directly the zero-field splitting constant, $D = 2.76 \pm 0.01 \text{ cm}^{-1}$.

To understand the origin of the magnetic anisotropy of Co^{2+} , we use and extend the standard crystal field (CF) theory [13, 17] and estimate the CF parameters. The Co^{2+} ion is in the d^7 configuration and Hund's rule coupling is sufficiently large to restrict the states essentially to $S = 3/2$, i.e. the 4F and 4P states. These states split due to the CF potential \hat{H}_{CF} and interact by spin-orbit coupling $\hat{H}_{\text{SO}} = \lambda \vec{L} \cdot \vec{S}$:

$$\hat{H} = \hat{H}_{\text{Coul}} + \hat{H}_{\text{CF}} + \hat{H}_{\text{SO}} \quad \hat{H}_{\text{CF}} = \hat{H}_{\text{cub}} + \hat{H}_{\text{trig}} \quad (2)$$

The 4P states are $15B$ higher in energy (B being the Racah parameter). The trigonal symmetry of the CF requires three parameters which, as in Refs. [17] and [18], we denote Δ , v , and v' .

The importance of the non-diagonal matrix element v' was first pointed out by MacFarlane [17] but was not

thoroughly treated in standard text books [13]. MacFarlane's formula [17] is a good approximation for strong cubic crystal fields ($\Delta \gg 15B$, as for Cr^{3+} complexes) but is not applicable in the present case where $15B \gg \Delta \gg v, v', \lambda$. Here, in order to calculate g_{\parallel} , g_{\perp} and D , we derive a perturbative formula for the parameters of the effective Hamiltonian ($g_s = 2.002$, k : reduction factor)

$$D = \frac{\lambda^2}{\Delta^2} \left[2v - \frac{10\sqrt{2}}{3} v' \left(1 + \frac{4}{75} \frac{\Delta}{B} \right) \right]$$

$$g_{\parallel} = g_s - \frac{8\lambda k}{\Delta} \left[1 - \frac{v}{3\Delta} + \frac{5\sqrt{2}}{9\Delta} v' \left(1 + \frac{4}{75} \frac{\Delta}{B} \right) \right] \quad (3)$$

$$g_{\perp} = g_s - \frac{8\lambda k}{\Delta} \left[1 + \frac{v}{6\Delta} - \frac{5\sqrt{2}}{18\Delta} v' \left(1 + \frac{4}{75} \frac{\Delta}{B} \right) \right].$$

Eq. (3) is more concise and hence more practicable than its counterpart derived in [19].

Numerical diagonalization of the Hamiltonian (2) within the subspace of the 4F and 4P states (a 40×40 matrix) yields the results shown in Table I. For the CF parameters obtained from optical measurements [18], the anisotropy and gyromagnetic factors agree very well with our measured values. For the same parameters the perturbative results of Eq. (3) are $g_{\parallel} = 2.27$, $g_{\perp} = 2.30$, and $2D = 4.34 \text{ cm}^{-1}$, and thus in good agreement with the numerical diagonalization.

| | EPR | optics | Harrison |
|-----------------|-------|--------|----------|
| Δ | | 4000 | 4000 |
| v | | -120 | 53 |
| v' | | -320 | -210 |
| g_{\parallel} | 2.236 | 2.24 | 2.21 |
| g_{\perp} | 2.277 | 2.28 | 2.23 |
| $2D$ | 5.52 | 4.04 | 3.14 |

TABLE I: Measured EPR data, compared to those calculated from CF theory with parameters from optics [18] or estimated from the Harrison approach. In all calculations the Racah parameter $B = 760 \text{ cm}^{-1}$ and the spin-orbit coupling $\lambda = -143.3 \text{ cm}^{-1}$ [18] were used. The energy unit is inverse centimeters.

To obtain more microscopic information about the CF parameters Δ , v and v' , we consider the hybridization contribution to the d -level splitting $E_m = (t_{pdm})^2 / \Delta_{pd}$, with the Slater-Koster hopping parameter t_{pdm} ($m = \sigma$ or π) parameterized according to Harrison [20, 21]. Adjusting the charge-transfer energy Δ_{pd} to the optical cubic splitting Δ gives $\Delta_{pd} = 3.6 \text{ eV}$ and $k = 0.85$ and leads to reasonable values of g_{\parallel} , g_{\perp} , and $2D$ (last column of Table I). So, we may give to the CF parameters that were derived from the optical measurements a microscopic foundation. Also, these parameters are very specific to the tetrahedral environment of Co with trigonal splitting which suggests that our experimental data can only

be explained if Co replaces Zn.

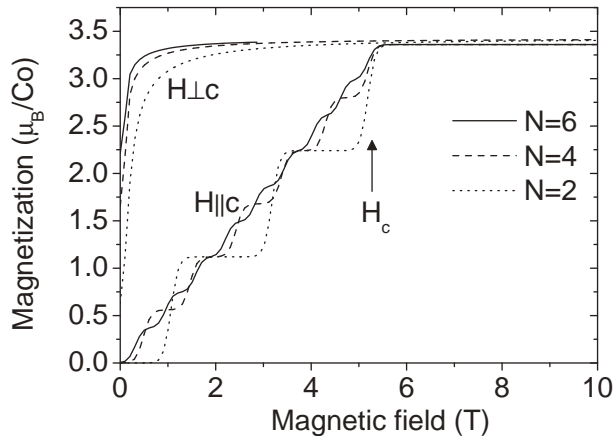


FIG. 4: Magnetization of FM Co^{2+} clusters ($N = 2, 4, 6$) as a function of the applied magnetic field, calculated at $T = 0.1\text{K}$ for $J = -21\text{cm}^{-1}$.

We finally discuss the possible magnetic states that would arise if the individual Co^{2+} ions in the ZnO lattice coupled ferromagnetically. This can be studied by adding a Heisenberg term ($\sum JS_iS_j$ with $J < 0$) to the Hamiltonian (1) [22]. The magnetization curves, obtained by exact numerical diagonalization of small $S = 3/2$ clusters (with $N = 2, 4, 6$), shown in Fig. 4, are rather insensitive to the exact value of the FM coupling, provided that $-J \gg D$. As can be seen from the figure, $M(H)$ strongly depends on the orientation of the magnetic field: for $H \perp c$, saturation is reached at very low fields; for $H \parallel c$, by contrast, the magnetization rises at first essentially linearly (for $N \gg 1$) and saturates only at a critical field, H_c . In the limit of $N \gg 1$, we have $g_{\parallel}\mu_B H_c = 2D$, and hence $\mu_0 H_c = 5.3\text{ T}$ for FM ZnO:Co. We also note that the saturated magnetization does not depend on the magnetic field orientation. To our knowledge the above described magnetic behavior has not been seen yet. In contrast to this prediction an "easy axis" magnetic anisotropy [23, 24, 25] or the absence of any anisotropy [6] were found in ferromagnetic polycrystalline ZnO:Co thin films, clearly indicating that Co electronic states other than $3d^7$ are responsible for the observed ferromagnetic signal.

In summary, we have presented an exhaustive study of the magnetic properties of Co-doped ZnO thin films in a low-concentration regime. Our experimental results and theoretical calculations clearly demonstrate a strong anisotropy of Co^{2+} ions in the ZnO lattice which affects the magnetic ground-state of ZnO:Co leading to an "easy plane" ferromagnet. In the absence of consensus regarding the magnetic properties of ZnO:Co we argue that the study of its magnetic anisotropy offers simple criteria,

both experimental and theoretical, for the identification of the intrinsic ferromagnetism in this material.

Financial support by the NATO science division (grant CLG 98 1255) is gratefully acknowledged.

-
- [1] I. Zutic, J. Fabian and D. Das Sarma, Rev. Mod. Phys. **76**, 324 (2004).
 - [2] J.K. Furdyna, J. Appl. Phys. **64**, R29 (1988); H. Ohno, Science **291**, 840 (2001); T. Dietl et al., Science **287**, 1019 (2000).
 - [3] K. Sato and H. Katayama-Yoshida, Physica E **10**, 251 (2001).
 - [4] A.S. Risbud et al., Phys. Rev. B **68**, 205202 (2003).
 - [5] E.-C. Lee and K.J. Chang, Phys. Rev. B **69**, 085205 (2004).
 - [6] W. Prellier et al., Appl. Phys. Lett. **82**, 3490 (2003).
 - [7] H.J. Lee et al., Appl. Phys. Lett. **81**, 4020 (2002).
 - [8] S.W. Lim, D.K. Hwang, J.M. Myoung, Sol. State. Comm. **125**, 231 (2003).
 - [9] D.P. Norton et al., Appl. Phys. Lett. **83**, 54 (2003). 205202 (2003).
 - [10] S.W. Yoon et al., J. Appl. Phys. **93**, 7879 (2003); S. Kolesnik, B. Dabrowski and J. Mais, J. Appl. Phys. **95**, 2582 (2004).
 - [11] J.H. Kim et al., Sol. State. Comm. **131**, 677 (2004).
 - [12] During our work on $\text{Zn}_{1-x}\text{Co}_x\text{O}$ a variety of epitaxial films with $x = 0.003 - 0.3$ have been fabricated and tested. We found that starting from $x=0.03-0.05$ AFM correlations between Co^{2+} determine the magnetic properties of these compounds. Therefore we believe that ZnO:Co is an intrinsically AFM material even when heavily electron doped ($n_e \geq 3 \cdot 10^{20}\text{ cm}^{-3}$).
 - [13] A. Abragam and B. Bleaney, *Electron Paramagnetic Resonance of Transition Ions*, Dover Publications (New York) 1986.
 - [14] T. Estle and M. De Wit, Bull. Am. Phys. Soc. **6**, 445 (1961).
 - [15] N. Jedrecy et al., Phys. Rev. B **69**, 041308(R) (2004).
 - [16] W.C. Holton, J. Schneider and T.L. Estle, Phys. Rev. **133A**, 1638 (1964).
 - [17] R. M. MacFarlane, J. Chem. Phys. **47**, 2066 (1967); Phys. Rev. B **1**, 989 (1970).
 - [18] P. Koidl, Phys. Rev. B **15**, 2493 (1977).
 - [19] Du Mao-Lu and Zhao Min-Guang, J. Phys. C : Solid State Phys. **21**, 1561 (1988).
 - [20] W. A. Harrison, *Electronic Structure and the Properties of Solids*, Freeman (San Francisco) 1980.
 - [21] M. D. Kuzmin, A. I. Popov, A. K. Zvezdin, Phys. stat. Sol. (b) **168**, 201 (1991).
 - [22] For the justification of the use of the isotropic exchange Hamiltonian in DMS see, for example, L. Brey and G. Gómez-Santos, Phys. Rev. B **68**, 115206. (2003).
 - [23] K. Rode et al., J. Appl. Phys. **93**, 7676 (2004).
 - [24] J. H. Park et al., Appl. Phys. Lett. **84**, 1338 (2004).
 - [25] A. Dinia et al., J. Appl. Phys. **97**, 123908 (2005).